

# Unsupervised Object-Level Video Summarization with Online Motion Auto-Encoder

Yujia Zhang, Xiaodan Liang, Dingwen Zhang, Min Tan, and Eric P. Xing

**Abstract**—Unsupervised video summarization plays an important role on digesting, browsing, and searching the ever-growing videos everyday. Despite the great progress achieved by prior works (e.g., the frame-level video summarization), the underlying fine-grained semantic and motion information (i.e., objects of interest and their key motions) in online videos has been barely touched, which is more essential and beneficial for many downstream tasks (e.g., object retrieval) in an intelligent system. In this paper, we investigate a pioneer research direction towards the fine-grained unsupervised object-level video summarization. It can be distinguished from existing pipelines in two aspects: extracting key motions of participated objects, and learning to summarize in an unsupervised and online manner that is more applicable for online growing videos. To achieve this goal, we propose a novel online motion Auto-Encoder (online motion-AE) framework that functions on the super-segmented object motion clips. The online motion-AE mimics the online dictionary learning for memorizing past states of object motions by continuously updating a tailored recurrent auto-encoder network. This online updating scheme enables the differentiable optimization of jointly online feature learning and dictionary learning to discriminate key object-motion clips. Finally, the key object-motion clips can be mined by using the reconstruction errors obtained by the online motion-AE. Comprehensive experiments on a newly-collected surveillance dataset and the public Base jumping, SumMe, and TVSum datasets have demonstrated the effectiveness of online motion-AE, and the application potential of fine-grained object-level video summarization.

**Index Terms**—Object-level video summarization, online motion Auto-Encoder, stacked sparse LSTM auto-encoder.

## I. INTRODUCTION

VIDEO has rapidly become one of the most common sources of visual information. The amount of online accessible video data is daunting with the success of mobile phones, activity cameras, Google Glass, etc. Consequently, automatic tools for analyzing and understanding video contents are essential for the large-scale intelligent system. In particular, automatic video content summarization techniques, e.g., [1]–[5], have received wide research interest in recent years due to its huge application potentials. The goal is to compactly depict the original video, distilling its important events into a short watchable synopsis.

Y. Zhang and M. Tan are with Institute of Automation, Chinese Academy of Sciences; School of Computer and Control Engineering, University of Chinese Academy of Sciences, Beijing, China. (email: zhangyujia2014@ia.ac.cn, min.tan@ia.ac.cn.) Work done while the first author was at CMU.

X. Liang and Eric P. Xing are with Machine Learning Department, Carnegie Mellon University, Pittsburgh, PA, USA. (email: xdliang328@gmail.com, epxing@cs.cmu.edu.)

D. Zhang is with School of Automation, Northwestern Polytechnical University, Xi'an, China. (e-mail: zdw2006yyy@mail.nwpu.edu.cn.)

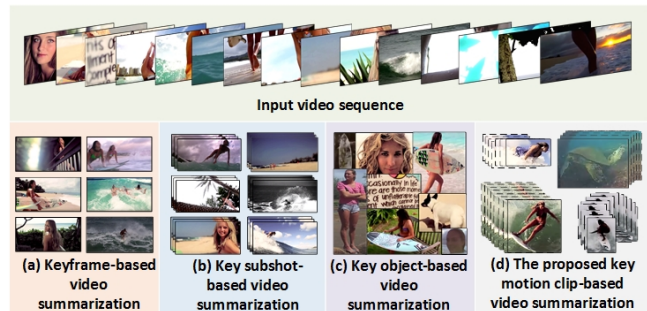


Fig. 1. Different types of video summarization techniques. Specifically, existing methods including (a) keyframe, (b) key subshot (c) key object-based (only spatial) video summarization. Our proposed unsupervised object-level (motion-clip based) video summarization technique (d) attempts to mine key object motion clips to compactly depict the whole video.

As shown in Fig. 1 (a)–(c), the existing video summarization techniques often shorten the input video mainly in three different ways, i.e., keyframe selection, key subshot selection, key object selection within frames, respectively. Specifically, the keyframe-based approaches (e.g. [4], [6]–[8]) generate the video summary comprised by a collection of key frames, while the key subshot-based approaches (e.g. [9]–[12]) select the representative subshots of frames to form the video summary. Recently, the key object-based approach [13] proposes to break down the whole video into several single frames that reveal the representative objects existing in a given video.

Despite the great progress achieved by the prior works, the underlying fine-grained semantic and motion information (i.e., objects of interest and their key motions) in online videos has been barely touched, which is more essential and beneficial for many downstream tasks (e.g., object retrieval) in an intelligent system. Besides, among the prior works, most of them (e.g., [14]–[16]) address the ill-posed supervised or semi-supervised video summarization with the requirement of predefining the patterns of key frames, which is impractical and not scalable to handle diverse and complicated ever-growing video contents.

To this end, this paper investigates a pioneer research direction towards the fine-grained unsupervised object-level video summarization as show in Fig. 1 (d) and Fig. 2. Such new video summarization can be distinguished from the existing ones mainly in two aspects: extracting key motions of participated objects and learning to summarize in an unsupervised and online manner that is more applicable for online growing videos. Compared with the conventional keyframe-based and key subshot-based approaches, the investigated



Fig. 2. The proposed unsupervised object-level video summarization attempts to mine key object motion clips to compactly depict the whole video. The dashed lines in the figure indicate the moving trajectories of the object instances in the extracted key object motion clips. Essentially, the video summaries generated by the proposed approach can not only answer the question of “what are the representative objects residing in the video?” but also answer “what attractable actions of these objects are occurring in the video?”

video summarization pipeline could realize more fine-grained video summarization, focusing on the foreground moving object instances rather than the entire image scenes. Compared with the key object-based approach, our method takes the temporal motion into consideration, which can better match the nature of the video sequence. Essentially, the video summaries generated by the proposed approach can not only answer the question of “what are the representative objects residing in the video?” but also answer “what attractable actions of these objects are occurring in the video?”

To achieve the goal of the fine-grained object-level video summarization, we propose a novel online motion Auto-Encoder (online motion-AE) framework that functions on the super-segmented object motion clips in an unsupervised way. Online motion-AE mimics the online dictionary learning for memorizing past states of object motions by continuously updating a tailored recurrent auto-encoder network, that is, a stacked sparse Long Short-Term Memory (LSTM) auto-encoder. This online updating scheme enables the differentiable optimization of jointly online feature learning and dictionary learning to discriminate key motion clips in an unsupervised manner for online growing videos.

The concrete framework as well as a brief illustration are shown in Fig. 3. More specifically, online motion-AE has the following merits. Firstly, in contrast with the previous supervised video summarization approaches like [14]–[16] that rely on the video dataset with human-created summary ground-truths for learning summarization models, the proposed approach does not require any annotations and yet is capable of automatically mining representative patterns of the object motion clips via an encoder-decoder mechanism. Secondly, rather than following several manually designed criteria to prioritize and select frames or subshots from videos as prior unsupervised video summarization methods [2], [6], [17] do, our model can learn an intrinsic measurement from the unsupervised reconstruction errors of our model to judge the distinctiveness of each object motion clip. Finally, compared with the group sparse coding approach for online summarization [5], our online motion-AE model can achieve both

the online updating of the encoded motion representation for each object motion clip and the adaptive adjustment of the reconstruction state by a unified deep LSTM encoder-decoder network.

In summary, this paper makes the following four-fold contributions:

- **Key object motion-based video summarization.** We explore a pioneer research direction towards the fine-grained unsupervised video summarization that dives into the key object motion clips of a video stream to compactly depict the whole video and generate video summaries.
- **Unsupervised online dictionary learning.** We propose a novel online motion-AE model, which can mimic the online dictionary learning for memorizing past states of object motions by continuously updating a tailored recurrent auto-encoder network. Such online updating scheme enables the differentiable optimization of the joint online feature learning and dictionary learning and thus can effectively discriminate the desired key object-motion clips.
- **The newly-collected OrangeVille benchmark.** A new surveillance video dataset is collected that allows for the objective evaluation of our new field of video summarization methods. We provide the spatial-temporal annotations for all key object motion clips to push forward the video summarization research with diverse granularities.
- **State-of-the-art performance for both object motion-level and frame-level summarization.** Besides the key object motion-based summarization comparison on OrangeVille, we also conduct comprehensive experiments on other existing video summarization benchmarks (the Base jumping, SumMe, and TVSum benchmark), and compare with several state-of-arts to demonstrate the effectiveness of the proposed approach.

## II. RELATED WORK

There are mainly four lines of the existing video summarization techniques, i.e., the keyframe-based approach, the key subshot-based approach, the key object-based approach, and others, respectively.

The keyframe-based video summarization methods [3], [4], [6], [7], [14], [17], [18] aim at identifying a series of discontinuous frames to form a summary that can represent the main video content well. For example, Mundur et al. [7] proposed to represent the video frame contents as multi-dimensional point data and use the Delaunay Triangulation-based clustering method to generate good quality summaries with fewer frames and less redundancy. Khosla et al. [6] used web-images as a prior to facilitate video summarization. The intuition is that people tend to take pictures of objects and events from a few canonical viewpoints in order to capture them in a maximally informative way. Kim et al. [4] achieved video summarization by diversity ranking on the similarity graphs between Flickr images and YouTube video frames. They formulated the storyline graphs as the inference of sparse time-varying directed graphs from a set of photo streams with assistance of videos.

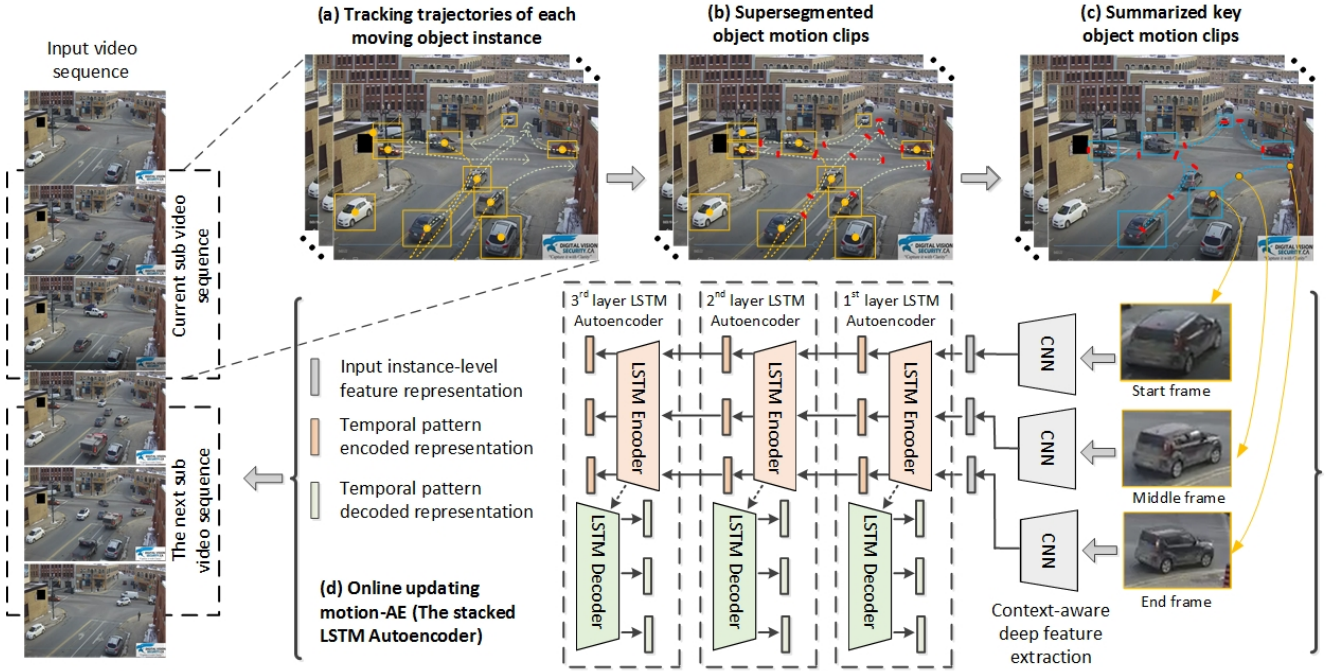


Fig. 3. The framework of the proposed online motion-AE model. Briefly, it sequentially reads and preprocesses each sub video sequence in an online manner. For each sub video sequence, we first track all the appearing object instances (as shown in (a)) and segment each of them into multiple object motion clips (as shown in (b)). Then, the deep LSTM auto-encoder obtained previously is adopted to select the key object motion clips in the current video sequence. Next, all the clips in the current video sequence are used to update the deep LSTM auto-encoder, which will be used in the next upcoming sub video sequence. Notice that the dashed arrows indicate the motion trajectories of the object instance. Specifically, the yellow/green dashed arrows in (a) and (b) indicate the motion trajectories before/after the current video frame shown in the figure. The blue ones in (c) indicate the motion trajectories of the summarized key motion clips. The red dots in (a), (b), and (c) indicate the separation point of adjacent object motion clips.

Different from the keyframe-based approaches, the key subshot-based video summarization approaches [9]–[11], [19], [20] aim at identifying a series of defining subshots, each of which is a temporally contiguous set of frames spanning a short time interval. For example, Yao et al. [20] presented highlight-driven based video summarization by exploring the moments of user interests. Specifically, they decomposed video segments into spatial and temporal streams to predict highlight score, and single out video segments which have the maximum sum of highlight scores. Song et al. [21] presented to use co-archetypal analysis technique to select shots which are most relevant to canonical visual concepts shared between video and images, according to the results of title-based image search. Zhang et al. [22] achieved video summarization via sparse coding with generalized sparse group lasso to learn a dictionary of video features and a dictionary of spatial-temporal feature correlation graphs, and thus informative segments can be generated. Laganire et al. [9] studied of spatial-temporal activity within the video and proposed to construct the final summary by selecting the clips showing the highest level of activity. Lu et al. [11] presented a video summarization approach that can discover the story of an egocentric video, which is based on a selection objective that captures the influence between subshots as well as shot importance and diversity. The method proposed by Zhang et al. [16] can implement video summarization either on the frame level or the subshot level. They designed a novel subset selection technique that can transfer summary structures from annotated videos to unseen

testing videos. More recently, Meng et al. [13] proposed to summarize the video content into a collection of key objects, leading to the key object-based video summarization. Specifically, they formulated this representative selection problem as a sparse dictionary selection problem, i.e., choosing a few representative object proposals to reconstruct the whole proposal pool, then proposed to incorporate object proposal prior and locality prior in the feature space when selecting representative objects. The summarized key objects can be potentially used to facilitate the understanding of the video content in object level. Besides the aforementioned video summarization manners, there are also some other interesting approaches, e.g. [23]–[27]. For example, Sun et al. [24] proposed to summarize video content by first finding the “montageable moments” and then identifying salient people and actions to depict in each montage. Pritch et al. [25] proposed to summarize an endless video (usually generated by webcams or surveillance cameras) by generating the corresponding video synopsis as a response to the users query. Zhang et al. [26] and Chu et al. [27] made attempt to summarize the related video content from a given video collection rather than a single video. Such methods can effectively mine the co-occurring spatial-temporal patterns across multiple related videos.

### III. ONLINE MOTION AUTO-ENCODER (ONLINE MOTION-AE)

The proposed online motion-AE framework resolves the fine-grained unsupervised video summarization problem by

training a stacked sparse LSTM auto-encoder in an online manner. In next sections, we first introduce the main stacked sparse LSTM auto-encoder module, and then present the details in building our online motion-AE framework.

#### A. The Stacked Sparse LSTM Auto-Encoder

The key towards the fine-grained unsupervised object-level video summarization is the model capability of capturing key object-level motion clips within each video. Inspired by the success achieved by recurrent neural networks (especially Long Shot-Term Memory (LSTM) [28]) on sequential modeling for images [29]–[31] and videos [32]–[35], our core learning module is established by plugging the hierarchical three LSTM layers into a generative auto-encoder model with the sparse constraint, as illustrated in Fig. 4. The sparse LSTM auto-encoder is thus able to learn the intrinsic motion patterns to reconstruct the input object sequence with the least possible amount of distortion. The learned parameters can be analogous to a compact “motion dictionary” of past observed object clips. Given a new object clip, we can easily judge its distinctness with respect to past ones by the reconstruction error induced from the learned LSTM auto-encoder model.

Specifically, the sparse LSTM auto-encoder model consists of a LSTM encoder and a LSTM decoder. The LSTM encoder recurrently takes each feature in the object clip as the input, and feed-forward it into the hierarchal LSTM layers at each time-step. After passing all features of the clip at all time-steps, a motion context vector is generated to encode the holistic temporal motion and appearance patterns. On the other hand, the LSTM decoder network decodes the extracted motion context vector by three symmetric LSTM layers to obtain a synthesized representation sequence. The sparse constraint is imposed on the encoded motion context vector to ensure the compactness and generalization capability of “the motion dictionary”. The reconstruction error between the synthesized features and input features is used as a measurement to determine whether this input sample has already been memorized by the recurrent auto-encoder. The unsupervised optimization of the sparse LSTM auto-encoder can be realized by the differential back-propagation algorithm to minimize the difference between the reconstructed features and input features. In the next, we will go through some details of the basic LSTM unit, the LSTM auto-encoder, the sparse LSTM auto-encoder, and the stacked sparse LSTM auto-encoder in order.

**LSTM Unit.** As shown in Fig. 4 (A), the basic LSTM unit, which is used for long-sequence modeling, applies a memory cell  $\mathbf{c}_t$  to record and encode the history of the knowledge of the inputs observed in previous time steps and determine the hidden cell in the current time step  $\mathbf{h}_t$ . Here, the memory cell  $\mathbf{c}_t$  and hidden cell  $\mathbf{h}_t$  are modulated by nonlinear gate functions (e.g., the forget gate, output gate, and input gate), which determine whether the LSTM keeps the values at the gates (if the gates evaluate to 1) or discard them (if the gates evaluate to 0) [36].

Specifically, there are three types of gates: the input gate ( $\mathbf{i}$ ) controls whether the LSTM considers its current input  $\mathbf{x}_t$ , the forget gate ( $\mathbf{f}$ ) allows the LSTM to forget its previous

memory  $\mathbf{c}_t$ , and the output gate ( $\mathbf{o}$ ) decides how much of the memory to transfer to the hidden states  $\mathbf{h}_t$ . These gates together lead to the ability on learning complex long-sequence modeling for LSTM. In particular, the forget gate ( $\mathbf{f}$ ) serves as a time-varying data-dependent on/off switch to selectively incorporating the past and present knowledge [37].

The concrete formulations are defined as:

$$\begin{aligned}\mathbf{i}_t &= \sigma(W_{ix}\mathbf{x}_t + \Phi_{ih}\mathbf{h}_{t-1} + \mathbf{b}_i), \\ \mathbf{f}_t &= \sigma(W_{fx}\mathbf{x}_t + \Phi_{fh}\mathbf{h}_{t-1} + \mathbf{b}_f), \\ \mathbf{o}_t &= \sigma(W_{ox}\mathbf{x}_t + \Phi_{oh}\mathbf{h}_{t-1} + \mathbf{b}_o), \\ \mathbf{c}_t &= \mathbf{i}_t \otimes \phi(W_{cx}\mathbf{x}_t + \Phi_{ch}\mathbf{h}_{t-1} + \mathbf{b}_c) + \mathbf{f}_t \otimes \mathbf{c}_{t-1}, \\ \mathbf{h}_t &= \mathbf{o}_t \otimes \phi(\mathbf{c}_t),\end{aligned}\quad (1)$$

where  $\sigma$  is a sigmoid function,  $\phi$  is the hyperbolic tangent function  $\tanh$ ,  $\otimes$  donates element-wise product,  $\mathbf{W} = \{W_{ix}, W_{fx}, W_{ox}, W_{cx}\}$  is the transform from the input to LSTM states,  $\Phi = \{\Phi_{ih}, \Phi_{fh}, \Phi_{oh}, \Phi_{ch}\}$  is the recurrent transformation matrix between the hidden states, and  $\mathbf{b}$  is the bias vector.

**LSTM Auto-Encoder.** In LSTM auto-encoder, both the encoder network and the decoder network are built upon the LSTM units. Given an input object clip  $\mathbf{X} = (\mathbf{x}_1, \dots, \mathbf{x}_T)$ , the LSTM encoder recurrently output hidden states  $(\mathbf{h}_1, \dots, \mathbf{h}_T)$  with shared network parameters  $\Theta^E = \{\mathbf{W}^E, \Phi^E, \mathbf{b}^E\}$ , where  $\mathbf{W}^E$  is the transform from the input to LSTM encoder states,  $\Phi^E$  is the recurrent transformation matrix between the encoder states, and  $\mathbf{b}^E$  is the encoder bias vector. Symmetrically, the LSTM decoder recurrently decodes hidden states with the shared network parameters  $\Theta^D = \{\mathbf{W}^D, \Phi^D, \mathbf{b}^D\}$ , and generates the current reconstruction output  $\mathbf{Y} = (\mathbf{y}_1, \dots, \mathbf{y}_T)$  via an additional linear mapping:

$$\mathbf{y}_t = W_{yh}\mathbf{h}'_t + \mathbf{b}_h, \quad (2)$$

where  $\{W_{yh}, \mathbf{b}_h\}$  are the reconstruction mapping parameters, and  $\mathbf{h}'_t$  is the hidden state inferred for reconstructing the  $t$ -th input feature.

Training the whole LSTM auto-encoder is to optimize the parameters  $\{\Theta^E, \Theta^D, W_{yh}, \mathbf{b}_h\}$  by minimizing the mean-squared reconstruction error between the input sequence and the corresponding reconstructed sequence via:

$$\arg \min_{\Theta^E, \Theta^D, W_{yh}, \mathbf{b}_h} \mathcal{L}(\mathbf{X}, \mathbf{Y}) = \frac{1}{2T} \sum_{t=1}^T \|\mathbf{x}_t - \mathbf{y}_t\|_2^2. \quad (3)$$

**Sparse LSTM Auto-Encoder.** Motivated by the physiological evidence that describing patterns with less active neurons minimizes the probability of destructive cross-talk [38], a regularization term is applied to constraining the sparsity to the target activation function [39], [40]. It penalizes a deviation of the expected activation of the hidden states representation from a fixed (low) level  $\rho$  by optimizing:

$$\begin{aligned}\arg \min_{\Theta^E, \Theta^D, W_{yh}, \mathbf{b}_h} \sum_{k=1}^K \mathcal{L}(\mathbf{X}^{(k)}, \mathbf{Y}^{(k)}) + \beta \sum_{d=1}^D KL(\rho || \hat{\rho}_d), \\ KL(\rho || \hat{\rho}_d) = \rho \log \frac{\rho}{\hat{\rho}_d} + (1 - \rho) \log \frac{(1 - \rho)}{(1 - \hat{\rho}_d)},\end{aligned}\quad (4)$$

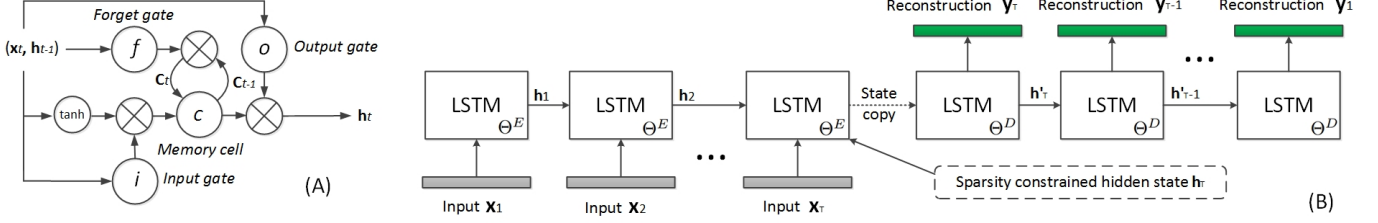


Fig. 4. The illustration of (A) the LSTM unit and (B) the sparse LSTM auto-encoder (B). LSTM unit is a type of recurrent neural network, which models long-range dependencies. Sparse LSTM auto-encoder is established by plugging the hierarchical three LSTM layers into a generative auto-encoder model with the sparse constraint.

where  $\mathbf{X}^{(k)}$  indicates the  $k$ -th training sample in the training set of totally  $K$  training sequences,  $D$  indicates the dimension of the hidden states,  $\rho$  is the target average activation of each dimension of the hidden state  $\mathbf{h}_T$ , and  $\hat{\rho}_d = \sum_{k=1}^K [h_T^{(k)}]_d / K$  is the average activation of the  $d$ -th dimension of the hidden state  $[h_T]_d$  over  $K$  training samples. The Kullback-Leibler (KL) divergence  $KL(\cdot)$  is used to impose the sparse constraint. As claimed in sparse coding [39], a non-redundant over-complete feature set can be learned when  $\rho$  is small. Here, we set  $\rho = 0.05$  as suggested in [39].

The architecture of a sparse LSTM auto-encoder network is shown in Fig. 4 (B), which is established by plugging the hierarchical three LSTM layers into a generative auto-encoder model with sparse constraint. Notice that the output reconstruction sequence are in reverse order as compared with the input sequence as suggested by [32], which could make the optimization easier because the model can get off the ground by looking at low range correlations.

**Stacked Sparse LSTM Auto-Encoder.** The final deep network is established by stacking  $M = 3$  sparse LSTM auto-encoder layers as shown in Fig. 3 (d). To achieve the hierarchical latent representation, the hidden states ( $\mathbf{h}_1, \dots, \mathbf{h}_T$ ) from the first (bottom) LSTM auto-encoder layer is posed as the input ( $\mathbf{x}_1, \dots, \mathbf{x}_T$ ) of the second LSTM auto-encoder layer. The dimension of hidden states in each LSTM layer is gradually decrease to capture more high-level motion representation by stacking more LSTM auto-encoder layers. Like many stacked auto-encoder models (e.g., [32], [40]), the proposed deep LSTM auto-encoder model can be easily trained (both in the offline training stage and the online updating stage) using greedy optimization: training each of the sparse LSTM auto-encoder layer one by one via optimizing the objective function (4) using stochastic gradient descent.

### B. Online Video Summarization

Aiming at the fine-grained video summarization that dives into object instances, our online learning framework incorporates the multiple object tracking and motion trajectory segmentation to extract candidate object motion clips, and then processes these clips with the stacked sparse LSTM auto-encoder model in an online manner.

1) *Preprocessing: Multiple Object Tracking.* We first track all moving objects in the video to discover all objects of interest to be summarized. Notice that the single object

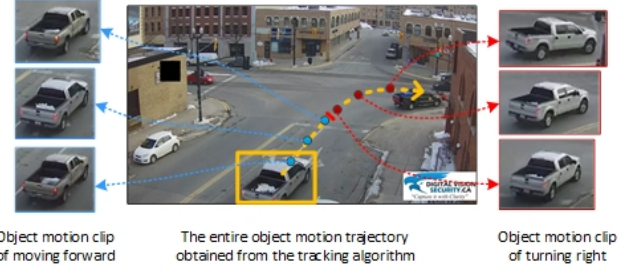


Fig. 5. An example of the motion trajectory segmentation. The motion trajectory of each object instance was super-segmented into multiple object motion clips, reflecting different motion status with unnoticeable changes.

tracking (SOT) techniques as used in some previous video understanding systems [41]–[43] cannot be readily used in our task as 1) they would miss many objects that are absent at the first frame of the video (or shot), and 2) they tend to be time-consuming when there are intensive objects appearing in the video (e.g., the surveillance video in our case).

Due to arbitrary number of objects that may appear in each frame, we adopt a state-of-the-art multiple object tracking algorithm, i.e., the Markov Decision Process (MDP) tracker [44], which is a tracking-by-detection algorithm equipped with effective tracking model in handling the appearance/disappearance of any object instance in the video. The lifetime of each object is modeled with a MDP describing the transitions between four subspaces of states (*active*, *tracked*, *inactive*, *lost*) which corresponds to seven actions. All deterministic actions are learned from reward functions to learn a policy which can maximize the total obtained rewards. Data association is learned by a similarity function which is as part of the MDP policy with reinforcement learning. In this way, it can benefit from the advantages of both offline and online learning. Particularly, the localization of moving objects is achieved by performing the pre-trained Faster RCNN [45] model on PASCAL VOC [46] dataset on down-sampled frames.

**Motion Trajectory Segmentation.** With the goal of finding the distinct motion patterns of each object, we thus super-segment the motion trajectory of each object instance into multiple object motion clips, each of which reflects a certain motion status with unnoticeable changes as shown in Fig. 5. One straight-forward way would be to cut each motion trajectory into clips within the fixed length. However, such

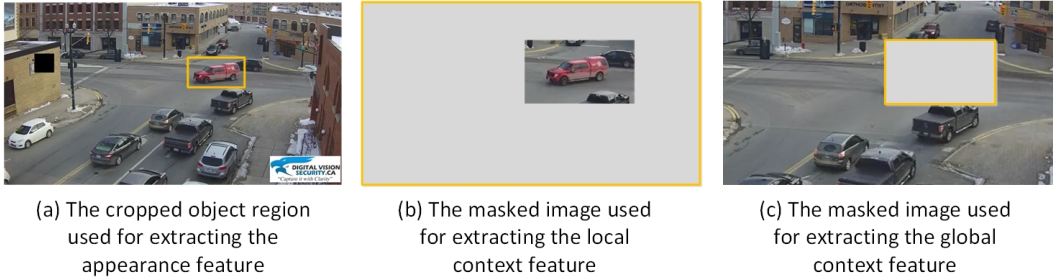


Fig. 6. Context-aware feature representation. The orange boxes are the bounding box locations feeding into the Faster RCNN to extract the corresponding features. (b) and (c) are global and local context-aware feature representation respectively.

arbitrarily cutting clips would destroy some continuous motion sequences. An alternative way is to use the shot detection approach [47], which is mainly based on changes in the color histogram. This still cannot work well in our case as the sequences formed by the cropped object trajectories usually contain the image regions with similar color distribution (see Fig. 5).

We thus adopt the recent superframe segmentation method [1], which cuts video sequences mainly based on the motion information by defining an energy function  $E(S_j)$  [1] for the measurement of a superframe  $S_j$ :

$$\begin{aligned} E(S_j) &= \frac{1}{1 + \gamma C_{cut}(S_j)} P_l(|S_j|), \\ C_{cut}(S_j) &= m_{in}(S_j) + m_{out}(S_j), \end{aligned} \quad (5)$$

where  $C_{cut}$  is the cut cost,  $\gamma$  controls the influence between cost and length prior  $P_l$ , and  $m_{in}$  and  $m_{out}$  are motion magnitude estimated in the first and last frame of each superframe respectively. Each long motion trajectory for each object is thus effectively split into several continuous motion clips with variable lengths.

**Context-aware Feature Representation.** Given the super-segmented motion clips, we extract the context-aware feature representation for each region as the inputs to sparse LSTM auto-encoder. Specifically, we consider a key object motion clip from two perspectives: the distinct object appearance and distinguished surrounding context. We thus represent each region with a 8192-dimension vector by concatenating the appearance feature and the context feature extracted by the Faster RCNN network [48]. Specifically, the appearance feature is the 4096-dimension feature vector generated by feeding the original object region into Faster RCNN network and using the “fc7” layer pooled from the corresponding object bounding box location (see Fig. 6 (a)). The context feature is another 4096-dimension feature vector generated by feeding the masked image, which is produced by replacing the pixel values out of the expanded bounding box<sup>1</sup> region with the fixed mean pixel values pre-computed on ILSVRC 2012 [49] into Faster RCNN network, and then using the “fc7” layer pooled from the entire image scene (see Fig. 6 (b)). This context-aware representation can not only capture the detailed

appearance of each moving object, but also its corresponding location and surrounding context.

2) *Offline Training Process:* The sparse LSTM auto-encoder model is first initialized with an offline learning process to obtain the basic reconstruction capability, which is then updated in an online way. Specifically, we first collect a 40-minute-long (with 83278 frames) video sequence as the offline training data. Then, we randomly extract 30 bounding boxes from each offline video frame and copy each bounding box three times to form a still object sequence. In this way, the offline learned model will have the knowledge information for still object sequence, and thus can better differentiate moving object clips. Afterwards, the context-aware feature of each still sequence are thus used to train the stacked sparse LSTM auto-encoder.

3) *Online Summarization Process:* Given each test video sequence, the proposed online motion-AE sequentially reads the video 1000 frames by 1000 frames, (i.e., each of the 1000-frame sequence is treated as the sub video sequence as shown in Fig. 3) and summarizes the key object motion clips. At each step, we first extract candidate object motion clips, and sample three object motion regions (i.e., the start, middle, and end regions) from the clip as the input to the stacked sparse LSTM auto-encoder. This down-sampling operation help significantly reduces the computational complexity and yet retains the informative temporal information. We then extract the context-aware feature representation (as introduced in III-B1) of the sampled object motion regions and use the pre-trained stacked sparse LSTM auto-encoder to obtain the reconstruction error of each object clip. Here the reconstruction errors can be naturally used as the summarization scores for unsupervised video summarization. Intuitively, key object motion clips with unseen appearance and motion cannot be well reconstructed from the patterns learned by either the offline video sequence or the previous video content in the online test video. Next, we use all clips in the current sub video sequence to update the stacked sparse LSTM auto-encoder for capturing the underlying motion patterns, and the updated network is employed on the upcoming sub video sequence. By performing the aforementioned online process for the whole video sequence, we can obtain the summarization score for each object motion clip, and thus get the final results for key object motion clip summaries.

<sup>1</sup>The bounding box is expanded to 2 times of its original length and width.

## IV. EXPERIMENT

### A. Experimental Settings

**Datasets.** We evaluate the performance of the proposed online motion-AE model on several datasets. The first one is the newly collected video surveillance dataset named as **OrangeVille**, which contains 30 surveillance video sequences downloaded from the YouTube website with the keyword of “OrangeVille” and filtering out the videos with low resolution and strong shadows. Each of the video in **OrangeVille** dataset averagely contains 3000 frames with the length of 100 seconds. The videos are recorded in outdoor scenes with moving objects mainly in categories of human, cars, buses, bicycles, and motorcycles. The motion/action of such objects are mainly *waiting*, *slow moving*, *fast moving*, and *turning around*. Targeting at the fine-grained object-level video summarization task that aims to discover all key object motion clips, we provide the spatial-temporal object bounding-box annotations to depict each key object motion clip in each video on **OrangeVille** dataset. The ground-truth annotations are labeled by a subject manually, focusing on the key object motions like fast moving cars, pedestrian crossing the road, and buses turning left/right.

The second dataset is the **Base jumping** dataset from public CoSum dataset [27]. Since CoSum dataset is applied for video co-summarization task, and the dataset is consisted of multiple videos organized into groups with topic keywords, we use one class of the whole dataset, i.e., the *Base jumping* class, to evaluate our model.

Besides, we also use other two frame-level datasets, which are the public **SumMe** dataset [1] and **TVSum** dataset [21]. Specifically, **SumMe** contains 25 videos covering *holidays*, *events* and *sports*, such as Statue of Liberty, saving dolphins and bike polo. **TVSum** contains 50 videos in 10 categories downloaded from YouTube defined in the TRECVID Multimedia Event Detection (MED). The contents in these two datasets are from both first-person and third-person videos, which addresses complex image scenes.

**Evaluation Metrics.** We adopted three common metrics, including the average precision (AP) score, the F-measure score, and the AUC score, which have been used in previous works (e.g., [15], [16]). The AP score were used to evaluate the generated summarization scores, which was generated by binarizing the samples via varying the quantification threshold within the range of [0, 1]. The resulting true positive rate (or the recall rate) versus precision rate at each threshold value formed the PR curve. Then the area under the PR curve was calculated as the AP score. Similarly, the AUC score was obtained by calculating the area under the ROC curve, which was generated based on the false positive rate and the true positive rate. Specifically, The precision  $PRE(Precision)$ , true positive rate  $TPR(Recall)$  and false positive rate  $FPR$  were defined as

$$\begin{aligned} PRE &= |SF \cap GF|/|SF|, \\ TPR &= |SF \cap GF|/|GF|, \\ FPR &= |SF \cap GB|/|GB|, \end{aligned} \quad (6)$$

where  $SF$ ,  $GF$  and  $GB$  denote the set of samples predicted as 1, the samples labeled as 1, and the samples labeled as 0, respectively. Different from AUC and AP, F-measure was adopted to evaluate the generated video summaries, which was defined as:

$$F = \frac{2Precision \times Recall}{Precision + Recall}. \quad (7)$$

During the evaluation process, the prediction results of the proposed approach as well as other compared state-of-the-art methods for the fine-grained object-level/frame-level video summarization tasks are the clip-level/frame-level real-valued scores ranging from 0 to 1 (after normalization). The AP scores and AUC scores can then be used to evaluate such real-valued prediction results directly. The F-measure scores were obtained by binarizing the predictions via a threshold  $\tau = 0.5$ .

In the fine-grained object-level video summarization task, the ground-truth are  $G$  human labeled object motion clips  $\{\mathbf{f}_g, \mathbf{b}_g^s, \mathbf{b}_g^e\}_{g=1}^G$ , where  $\mathbf{f}_g, \mathbf{b}_g^s$ , and  $\mathbf{b}_g^e$  indicate the temporal location (i.e., the frame numbers) of the  $g$ -th ground-truth clip, the spatial location (i.e., the object bounding box) in the start of the frame, and the spatial location in the end of the frame, respectively. Given an object motion clip  $\{\mathbf{f}_p, \mathbf{b}_p^s, \mathbf{b}_p^e\}$  which is predicted by the summarization algorithm, we calculate the IOU overlaps both for the spatial locations and the temporal locations as:

$$\begin{aligned} IOU^{tem} &= \frac{\mathbf{f}_p \cap \mathbf{f}_g}{\mathbf{f}_p \cup \mathbf{f}_g}, \\ IOU^{spa} &= \frac{1}{2} \left( \frac{\mathbf{b}_p^s \cap \mathbf{b}_g^s}{\mathbf{b}_p^s \cup \mathbf{b}_g^s} + \frac{\mathbf{b}_p^e \cap \mathbf{b}_g^e}{\mathbf{b}_p^e \cup \mathbf{b}_g^e} \right). \end{aligned} \quad (8)$$

Then, the object motion clips would be considered as correct summarization if  $IOU^{tem}$  and  $IOU^{spa}$  are simultaneously larger than the threshold  $\varphi$ . Due to the limited accuracy of the object tracking and superframe segmentation algorithms, we set  $\varphi = 0.1$  during our evaluation.

In the frame-level video summarization task, the ground-truths are the binary labels for each superframe provided by the dataset, while the prediction results are the predicted summarization scores for those superframes. In this case, all the evaluation metrics can be easily calculated because the temporal locations of all the test superframes are finely aligned with the corresponding ground-truths.

**Implementation Details.** We implemented our model on the public TensorFlow platform. The dimensions of hidden states of the first, second, and third sparse LSTM auto-encoder layers were 4096, 2048, and 1024, respectively. In the offline pre-training phase, we set the batch size as 100, while in the online updating phase, the batch size was dynamically determined by the number of clips extracted in each sub video sequence. The learning rate was set to 0.001 during the offline pre-training while 0.0001 during the online updating.

### B. Fine-Grained Video Summarization

In this section, we conducted extensive evaluation on fine-grained object-level video summarization task on **OrangeVille** dataset.

TABLE I  
COMPARISON OF THE FINE-GRAINED VIDEO SUMMARIZATION RESULTS BETWEEN THE PROPOSED APPROACH AND OTHER BASELINES ON THE **ORANGEVILLE** DATASET IN TERMS OF AUC SCORE, AP SCORE, AND F-MEASURE (HIGHER VALUES INDICATE BETTER RESULTS).

|           | Sparse [5]<br>Coding | Stacked Sparse Auto-Encoder [39] |          |          | Stacked LSTM Auto-Encoder [32] |          |          | Stacked Sparse LSTM Auto-Encoder(ours) |          |               |
|-----------|----------------------|----------------------------------|----------|----------|--------------------------------|----------|----------|--|----------|---------------|
|           |                      | 1 layer                          | 2 layers | 3 layers | 1 layer                        | 2 layers | 3 layers | 1 layer                                | 2 layers | 3 layers      |
| AUC score | 0.4252               | 0.4512                           | 0.4040   | 0.4354   | 0.4829                         | 0.5413   | 0.5680   | 0.4970                                 | 0.5598   | <b>0.5908</b> |
| AP score  | 0.1542               | 0.1615                           | 0.1493   | 0.1705   | 0.2177                         | 0.2476   | 0.2638   | 0.2275                                 | 0.2796   | <b>0.2850</b> |
| F-measure | 0.1284               | 0.1325                           | 0.1420   | 0.1662   | 0.2310                         | 0.2546   | 0.2795   | 0.2364                                 | 0.2721   | <b>0.2901</b> |

TABLE II  
COMPARISON OF DIFFERENT MASKS WHICH IS USED TO EXTRACT CONTEXT FEATURES ON STACKED SPARSE LSTM AUTO-ENCODER MODELS IN TERMS OF AUC SCORE, AP SCORE, AND F-MEASURE (HIGHER VALUES INDICATE BETTER RESULTS).

|           | mask = zero |          |          | mask = mean |          |               |
|-----------|-------------|----------|----------|-------------|----------|---------------|
|           | 1 layer     | 2 layers | 3 layers | 1 layer     | 2 layers | 3 layers      |
| AUC score | 0.4706      | 0.5178   | 0.5775   | 0.4970      | 0.5598   | <b>0.5908</b> |
| AP score  | 0.2008      | 0.2166   | 0.2420   | 0.2275      | 0.2796   | <b>0.2850</b> |
| F-measure | 0.1841      | 0.1886   | 0.1996   | 0.2364      | 0.2721   | <b>0.2901</b> |

TABLE III  
COMPARISON OF DIFFERENT FEATURES ON STACKED SPARSE LSTM AUTO-ENCODER MODELS IN TERMS OF AUC SCORE, AP SCORE, AND F-MEASURE (HIGHER VALUES INDICATE BETTER RESULTS).

|           | global + local |          |          | object + global |          |          | object + local |          |               |
|-----------|----------------|----------|----------|-----------------|----------|----------|----------------|----------|---------------|
|           | 1 layer        | 2 layers | 3 layers | 1 layer         | 2 layers | 3 layers | 1 layer        | 2 layers | 3 layers      |
| AUC score | 0.4889         | 0.4712   | 0.5175   | 0.4628          | 0.4857   | 0.5018   | 0.4970         | 0.5598   | <b>0.5908</b> |
| AP score  | 0.1928         | 0.1934   | 0.2026   | 0.1677          | 0.1834   | 0.1864   | 0.2275         | 0.2796   | <b>0.2850</b> |
| F-measure | 0.1839         | 0.1764   | 0.1362   | 0.1050          | 0.1216   | 0.1404   | 0.2364         | 0.2721   | <b>0.2901</b> |

TABLE IV  
COMPARISON OF THE NUMBER OF ONLINE UPDATES ON STACKED SPARSE LSTM AUTO-ENCODER MODELS IN TERMS OF AUC SCORE, AP SCORE, AND F-MEASURE (HIGHER VALUES INDICATE BETTER RESULTS).

|           | 1 online update |          |          | 2 online updates |          |               | 3 online updates |          |          |
|-----------|-----------------|----------|----------|------------------|----------|---------------|------------------|----------|----------|
|           | 1 layer         | 2 layers | 3 layers | 1 layer          | 2 layers | 3 layers      | 1 layer          | 2 layers | 3 layers |
| AUC score | 0.4427          | 0.5359   | 0.5826   | 0.4970           | 0.5598   | <b>0.5908</b> | 0.5268           | 0.5491   | 0.5710   |
| AP score  | 0.2084          | 0.2577   | 0.2801   | 0.2275           | 0.2796   | <b>0.2850</b> | 0.2369           | 0.2695   | 0.2630   |
| F-measure | 0.2228          | 0.2408   | 0.2684   | 0.2364           | 0.2721   | <b>0.2901</b> | 0.2414           | 0.2539   | 0.2157   |

**Comparison with state-of-the-art and baseline learning models.** To demonstrate the superiority of the proposed online motion-AE, we conducted comparisons with two state-of-the-art of the learning models, which are the online sparse coding as used in [5] and the stacked sparse auto-encoder as introduced in [39], respectively. Particularly, the online sparse coding proposed in [5] is one of the current state-of-the-art model for frame-level video summarization both in the online and unsupervised fashion. Other state-of-the-art video summarization approaches cannot be readily used in our comparison as they do not work in the unsupervised and online manner.

As for the online sparse coding-based approach, we firstly used the extracted object motion clips in the offline video sequence to learn a dictionary. Then, in the online testing phase, we used the previously constructed dictionary to calculate the reconstruction error for each new object motion clip in the current sub video sequence. We adopted the same motion-trajectory segmentation and context-aware feature representation modules used in our model to enable a fair comparison of different learning approaches. As for the state-of-the-art model of the stacked sparse auto-encoder, it can be implemented by

simply replacing the LSTM units with a single non-linear layer in our model.

The qualitative evaluation results are shown in Fig. 7, from which we can observe that the proposed online motion-AE can effectively summarize the key object motion clips, e.g., the fast driving cars, the occasionally appeared walkers who are crossing the road and turning around in the surveillance video sequence. Whereas the stacked sparse auto-encoder and sparse coding-based approaches are more likely to select non-key object motion clips, e.g., the stationary cars waiting for the traffic lights.

The quantitative evaluation results are shown in Table I. We can observe that the auto-encoder based models can significantly outperform the online sparse coding methods, even with a single layer, which demonstrates the good reconstruction capability of auto-encoders.

We also made comparisons with several model variants to show the effectiveness of each model component: 1) the stacked LSTM auto-encoder that eliminates the sparsity on the hidden states in each layer; 2) the shallow LSTM auto-encoder with or without using the sparse constraint, which only adopts one single LSTM auto-encoder layer to generate



TABLE V  
COMPARISON OF THE NUMBER OF LAYERS ON STACKED SPARSE LSTM AUTO-ENCODER MODELS IN TERMS OF AUC SCORE, AP SCORE, AND F-MEASURE (HIGHER VALUES INDICATE BETTER RESULTS).

|           | 1 layer | 2 layers | 3 layers      | 4 layers | 5 layers |
|-----------|---------|----------|---------------|----------|----------|
| AUC score | 0.4970  | 0.5598   | <b>0.5908</b> | 0.5919   | 0.5875   |
| AP score  | 0.2275  | 0.2796   | <b>0.2850</b> | 0.2582   | 0.2719   |
| F-measure | 0.2364  | 0.2721   | <b>0.2901</b> | 0.2712   | 0.2612   |



Fig. 7. Some examples of the fine-grained summarization results on the OrangeVille dataset. This shows the comparisons of our online motion-AE model with sparse coding [5] and stacked sparse auto-encoder [39] models.

reconstruction errors; 3) the two-layer LSTM auto-encoder models with or without the sparse constraint. From the obtained experimental results, it can be observed that using hierarchical LSTM auto-encoder structure as our full model can achieve better performance than the other variants that only adopt one or two layers. This is due to the more powerful hierarchical feature representations learned by our model, which can benefit for capturing complex object motion patterns.

**Ablation analysis.** We discuss different components in our stacked sparse LSTM auto-encoder model including the mask for extracting context feature, different types of feature representation, the number of online updates during testing phase and the number of layers for the stacked sparse LSTM auto-encoder model:

1) the mask we used to extract context features, one is produced by replacing the pixel values out of the expanded bounding box region with the fixed mean pixel values which are pre-computed on ILSVRC 2012 [48], and the other uses value of zero to replace the original pixel values. As shown in Table II, we can see that using mask of mean pixel value performs better than mask of zero value in all layers, since the settings for testing is the same as the one for training when using the mask of the fixed mean pixel value;

2) the different types of features we used for object motion clip feature representation, including the concatenating the global context and local context features (*global+local*), the

appearance feature and global context feature (*object+global*), and the appearance feature and local context feature (*object+local*). The way we concatenated feature is to just link the two 4096-dimensional feature vectors together to get the final 8192-dimensional feature vector. The global and local context feature are illustrated in Fig. 6 (b)(c). The results are shown in Table III, and we can observe that local context-aware feature have better representation ability, due to the reason that local context preserves and highlights the moving regions while global context would weaken motion information for the moving objects, and combining two different types of features also enhances the representative abilities of the model;

3) the number of online updates we used to update the stacked sparse LSTM auto-encoder model during testing period. We test our model by replacing different layers of sparse LSTM auto-encoder. From Table IV, we can see that using 1 and 2 online updates, the performance increases as the layers increase, but the performance decreases for 3 online updates due to the reason of over-learning;

4) the number of layers we used in our model. The results in Table V demonstrate that the stacked sparse LSTM auto-encoder often converges in the 3-rd layer and then would slightly decline with 4, 5 and more layers, so we use 3-layer stacked sparse LSTM auto-encoder model to learn the representation of features on object motion clips and compute reconstruction error for video summaries.



Fig. 8. Some examples of the frame-level summarization results on the Base jumping dataset. This shows the comparisons of our online motion-AE model with sparse coding [5] and stacked sparse auto-encoder [39] models.

### C. Frame-level Video Summarization

We demonstrate the generalization capability of our model on frame-level video summarization task, which is evaluated on the **Base jumping**, **SumMe** and **TVSum** datasets.

**Our tailored pipeline for frame-level summarization on Base jumping dataset.** We adapt our model for frame-level summarization, where the summarization scores of a certain frame was obtained by averaging the reconstruction errors of all object motion clips residing in it. In this way, the proposed approach as well as the baseline methods can be conveniently extended to obtain the frame-level summarization results.

The qualitative evaluation results are shown in Fig. 8, from which we can see that the proposed online motion-AE can summarize the key superframes that contain representative object motion, e.g., the moment for the jumping and flying. Whereas the stacked sparse auto-encoder and sparse coding-based approaches are more likely to select superframes with less informative object motion.

**Our tailored pipeline for frame-level summarization on SumMe and TVSum datasets.** We adapt our model for frame-level summarization, where the summarization scores of a certain superframe was obtained first by adopting the recent superframe segmentation method [1] to super-segment each video into multiple superframes, which cuts video sequences mainly based on the motion information. Then we used pre-trained ResNet152 [50] model on ILSVRC 2015 [51] to extract superframe motion features. After that, we used our online motion-AE model to obtain the reconstruction errors of all frame-level motion clips. In this way, the proposed approach as well as the baseline methods can be conveniently extended to obtain the frame-level summarization results. From the summarization results of **SumMe** and **TVSum** datasets in Fig. 9 and Fig. 10, we can see that the our online motion-AE model can effectively capture the informative and temporal motion patterns and thus obtain good results.

TABLE VI  
COMPARISON OF THE FRAME-LEVEL VIDEO SUMMARIZATION RESULTS BETWEEN THE PROPOSED APPROACH AND OTHER *Unsupervised* BASELINES ON **SUMMe** DATASET IN TERMS OF AUC SCORE, AP SCORE, AND F-MEASURE (HIGHER VALUES INDICATE BETTER RESULTS).

| Method                        | F_measure    |
|-------------------------------|--------------|
| Video MMR [52]                | 0.266        |
| TVSum [21]                    | 0.266        |
| VSUMM <sub>1</sub> [53]       | 0.328        |
| VSUMM <sub>2</sub> [53]       | 0.337        |
| stacked GRU Auto-Encoder [54] | 0.354        |
| <b>Online Motion-AE</b>       | <b>0.377</b> |

TABLE VII  
COMPARISON OF THE FRAME-LEVEL VIDEO SUMMARIZATION RESULTS BETWEEN THE PROPOSED APPROACH AND OTHER *Unsupervised* BASELINES ON **TVSum** DATASET IN TERMS OF AUC SCORE, AP SCORE, AND F-MEASURE (HIGHER VALUES INDICATE BETTER RESULTS).

| Method                        | F_measure    |
|-------------------------------|--------------|
| Web Image Prior [6]           | 0.360        |
| LiveLight [5]                 | 0.460        |
| TVSum [21]                    | 0.500        |
| stacked GRU Auto-Encoder [54] | 0.510        |
| <b>Online Motion-AE</b>       | <b>0.515</b> |

**Comparison with competitive learning models.** The quantitative evaluation results for **SumMe** and **TVSum** datasets are shown in Table VI and Table VII respectively. The state-of-arts we choose are all unsupervised methods, which are the same of our experimental settings for fair comparisons. As can be seen, the proposed stacked sparse LSTM auto-encoder again obtains better performance than other unsupervised baselines on two different datasets. This demonstrates that the proposed learning model can effectively capture the informative temporal motion patterns and thus obtain the outperforming performance. The performance gaps among different approaches become smaller as compared with those in the fine-grained



Fig. 9. Some examples of the frame-level summarization results on the SumMe dataset using our online motion-AE model. This shows some summary results from three videos in the dataset.

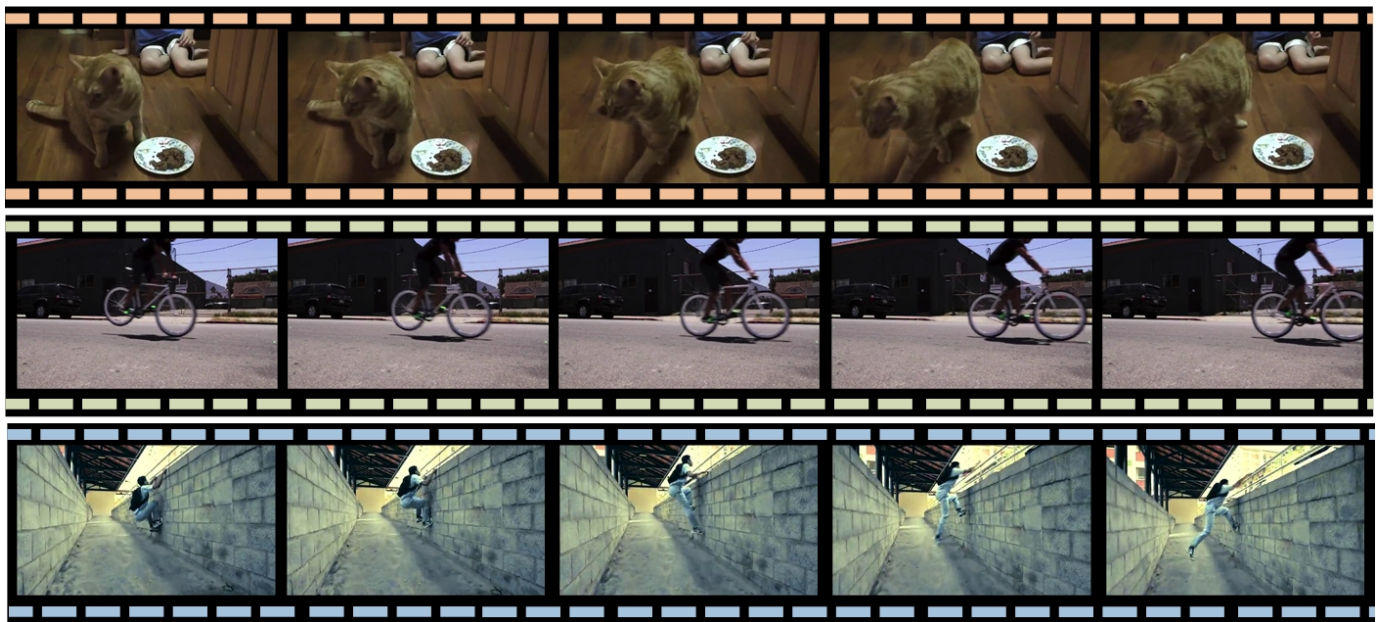


Fig. 10. Some examples of the frame-level summarization results on the TVSum dataset using our online motion-AE model. This shows some summary results from three videos in the dataset.

video summarization task. The reason is that the fine-grained video summarization requires the model be able to capture detailed instance-level motion patterns, which is much more challenging than the frame-level summarization task.

**Underlying connections between the two tasks.** Compared with the key object-motion clips summarized by the fine-grained object-level video summarization, the key frames summarized by the frame-level video summarization consider not only the distinct foreground object motions but also the attractive whole image scenes. Thus, generating the frame-level

summaries by only mining distinct object motion may partially cover the desired summarization result, which explains the performance gaps drop on the **SumMe** and **TVSum** datasets. We can observe that the performance drop of the proposed online motion-AE is not quite significant, which indicates that key object motions may actually occupy a relatively large portion of the factors in selecting frame-level summaries. Consequently, this demonstrates the potential usage of the fine-grained object-level video summarization approach.

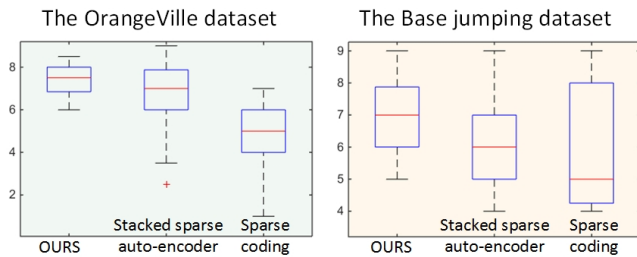


Fig. 11. The boxplot of the user study results on the collected OrangeVille dataset and the public Base jumping dataset on our online motion-AE model, stacked sparse auto-encoder [39] and sparse coding [5] models.

#### D. User Study

We further provide human evaluation results on **OrangeVille** and **Base jumping** datasets to better verify the model capability. Similar with [6], 15 subjects are asked to watch the randomly selected videos at 3x speed and then showed them the corresponding video summaries generated by different approaches. They were asked to rate the overall quality of each summarization result by assigning a rating from 1 to 10 (higher is better). The user study results on the **OrangeVille** dataset are reported in Fig. 11. Consistent with the objective evaluation results obtained by the evaluation metrics, our approach can consistently outperforms the stacked sparse auto-encoder and sparse coding models on the fine-grained object-level video summarization task. In addition, from the user study results, it can be seen that the proposed model can obtain more consistent subjective evaluation scores across different subject judges than the competitive models. Thus, this experiment further verifies the effectiveness of the proposed online motion-AE model.

#### V. CONCLUSION

In this paper, we investigated a pioneer research direction towards the unsupervised object-level video summarization. By diving into the fine-grained moving object instances residing in each given video sequence, the proposed online motion-AE approach can learn to summarize the extracted object motion clips in an unsupervised and online manner. Specifically, the online motion-AE can mimic the online dictionary learning for memorizing past states of object motions by continuously updating a tailored recurrent auto-encoder network, which enables the jointly online feature learning and dictionary learning to discriminate key motion clips. Comprehensive experiments on a newly collected **OrangeVille** dataset as well as public **Base jumping**, **SumMe** and **TVSum** datasets have demonstrated the effectiveness of the proposed approach both in the fine-grained video summarization and its application potential in the frame-level video summarization.

For future work, we plan to introduce the computational attention schemes [55]–[57] to improve the video summarization performance. On the other hand, we will apply the video summarization technique for assisting some high-level video understanding tasks like video object detection [58] and video prediction [59].

#### ACKNOWLEDGMENT

This project is supported by the Department of Defense under Contract No. FA8702-15-D-0002 with Carnegie Mellon University for the operation of the Software Engineering Institute, a federally funded research and development center.

#### REFERENCES

- [1] M. Gygli, H. Grabner, H. Riemenschneider, and L. Van Gool, “Creating summaries from user videos,” in *European conference on computer vision*, 2014, pp. 505–520.
- [2] D. Potapov, M. Douze, Z. Harchaoui, and C. Schmid, “Category-specific video summarization,” in *European conference on computer vision*, 2014, pp. 540–555.
- [3] Y. J. Lee, J. Ghosh, and K. Grauman, “Discovering important people and objects for egocentric video summarization,” in *Proceedings of the IEEE Conference on Computer Vision and Pattern Recognition*, 2012, pp. 1346–1353.
- [4] G. Kim, L. Sigal, and E. P. Xing, “Joint summarization of large-scale collections of web images and videos for storyline reconstruction,” in *Proceedings of the IEEE Conference on Computer Vision and Pattern Recognition*, 2014, pp. 4225–4232.
- [5] B. Zhao and E. P. Xing, “Quasi real-time summarization for consumer videos,” in *Proceedings of the IEEE Conference on Computer Vision and Pattern Recognition*, 2014, pp. 2513–2520.
- [6] A. Khosla, R. Hamid, C.-J. Lin, and N. Sundaresan, “Large-scale video summarization using web-image priors,” in *Proceedings of the IEEE Conference on Computer Vision and Pattern Recognition*, 2013, pp. 2698–2705.
- [7] P. Mundur, Y. Rao, and Y. Yesha, “Keyframe-based video summarization using delaunay clustering,” *International Journal on Digital Libraries*, vol. 6, no. 2, pp. 219–232, 2006.
- [8] A. A. Tonge and S. D. Thepade, “Key frame extraction for video content summarization using orthogonal transforms and fractional energy coefficients,” in *Proceedings of the IEEE conference on Information Processing*, 2015, pp. 642–646.
- [9] R. Laganière, R. Bacco, A. Hocevar, P. Lambert, G. Païs, and B. E. Ionescu, “Video summarization from spatio-temporal features,” in *Proceedings of the 2nd ACM TRECVID Video Summarization Workshop*, 2008, pp. 144–148.
- [10] J. Nam and A. H. Tewfik, “Event-driven video abstraction and visualization,” *Multimedia Tools and Applications*, vol. 16, no. 1, pp. 55–77, 2002.
- [11] Z. Lu and K. Grauman, “Story-driven summarization for egocentric video,” in *Proceedings of the IEEE Conference on Computer Vision and Pattern Recognition*, 2013, pp. 2714–2721.
- [12] Y.-L. Lin, V. I. Morariu, and W. Hsu, “Summarizing while recording: Context-based highlight detection for egocentric videos,” in *Proceedings of the IEEE International Conference on Computer Vision Workshops*, 2015, pp. 51–59.
- [13] J. Meng, H. Wang, J. Yuan, and Y.-P. Tan, “From keyframes to key objects: Video summarization by representative object proposal selection,” in *Proceedings of the IEEE Conference on Computer Vision and Pattern Recognition*, 2016, pp. 1039–1048.
- [14] B. Gong, W.-L. Chao, K. Grauman, and F. Sha, “Diverse sequential subset selection for supervised video summarization,” in *Advances in Neural Information Processing Systems*, 2014, pp. 2069–2077.
- [15] M. Gygli, H. Grabner, and L. Van Gool, “Video summarization by learning submodular mixtures of objectives,” in *Proceedings of the IEEE Conference on Computer Vision and Pattern Recognition*, 2015, pp. 3090–3098.
- [16] K. Zhang, W.-L. Chao, F. Sha, and K. Grauman, “Summary transfer: Exemplar-based subset selection for video summarization,” in *Proceedings of the IEEE Conference on Computer Vision and Pattern Recognition*, 2016, pp. 1059–1067.
- [17] D. Liu, G. Hua, and T. Chen, “A hierarchical visual model for video object summarization,” *IEEE transactions on pattern analysis and machine intelligence*, vol. 32, no. 12, pp. 2178–2190, 2010.
- [18] Y.-F. Ma, L. Lu, H.-J. Zhang, and M. Li, “A user attention model for video summarization,” in *Proceedings of the tenth ACM international conference on Multimedia*, 2002, pp. 533–542.
- [19] C.-W. Ngo, Y.-F. Ma, and H.-J. Zhang, “Automatic video summarization by graph modeling,” in *Proceedings of the IEEE international conference on computer vision*, 2003, pp. 104–109.

- [20] T. Yao, T. Mei, and Y. Rui, "Highlight detection with pairwise deep ranking for first-person video summarization," in *Proceedings of the IEEE Conference on Computer Vision and Pattern Recognition*, 2016, pp. 982–990.
- [21] Y. Song, J. Vallmitjana, A. Stent, and A. Jaimes, "Tvsum: Summarizing web videos using titles," in *Proceedings of the IEEE Conference on Computer Vision and Pattern Recognition*, 2015, pp. 5179–5187.
- [22] S. Zhang, Y. Zhu, and A. K. Roy-Chowdhury, "Context-aware surveillance video summarization," *IEEE Transactions on Image Processing*, vol. 25, no. 11, pp. 5469–5478, 2016.
- [23] F. Zhou, S. Bing Kang, and M. F. Cohen, "Time-mapping using space-time saliency," in *Proceedings of the IEEE Conference on Computer Vision and Pattern Recognition*, 2014, pp. 3358–3365.
- [24] M. Sun, A. Farhadi, B. Taskar, and S. Seitz, "Salient montages from unconstrained videos," in *European Conference on Computer Vision*, 2014, pp. 472–488.
- [25] Y. Pritch, A. Rav-Acha, A. Gutman, and S. Peleg, "Webcam synopsis: Peeking around the world," in *Proceedings of the IEEE international conference on computer vision*, 2007, pp. 1–8.
- [26] D. Zhang, J. Han, L. Jiang, S. Ye, and X. Chang, "Revealing event saliency in unconstrained video collection," *IEEE Transactions on Image Processing*, vol. 26, no. 4, pp. 1746–1758, 2017.
- [27] W.-S. Chu, Y. Song, and A. Jaimes, "Video co-summarization: Video summarization by visual co-occurrence," in *Proceedings of the IEEE Conference on Computer Vision and Pattern Recognition*, 2015, pp. 3584–3592.
- [28] S. Hochreiter and J. Schmidhuber, "Long short-term memory," *Neural computation*, vol. 9, no. 8, pp. 1735–1780, 1997.
- [29] X. Liang, X. Shen, D. Xiang, J. Feng, L. Lin, and S. Yan, "Semantic object parsing with local-global long short-term memory," in *Proceedings of the IEEE Conference on Computer Vision and Pattern Recognition*, 2016, pp. 3185–3193.
- [30] X. Liang, X. Shen, J. Feng, L. Lin, and S. Yan, "Semantic object parsing with graph lstm," in *European Conference on Computer Vision*, 2016, pp. 125–143.
- [31] X. Liang, L. Lin, X. Shen, J. Feng, S. Yan, and E. P. Xing, "Interpretable structure-evolving lstm," *arXiv preprint arXiv:1703.03055*, 2017.
- [32] N. Srivastava, E. Mansimov, and R. Salakhudinov, "Unsupervised learning of video representations using lstms," in *International Conference on Machine Learning*, 2015, pp. 843–852.
- [33] P. Pan, Z. Xu, Y. Yang, F. Wu, and Y. Zhuang, "Hierarchical recurrent neural encoder for video representation with application to captioning," in *Proceedings of the IEEE Conference on Computer Vision and Pattern Recognition*, 2016, pp. 1029–1038.
- [34] G. Li, S. Ma, and Y. Han, "Summarization-based video caption via deep neural networks," in *Proceedings of the 23rd ACM international conference on Multimedia*, 2015, pp. 1191–1194.
- [35] H. Yang, B. Wang, S. Lin, D. Wipf, M. Guo, and B. Guo, "Unsupervised extraction of video highlights via robust recurrent auto-encoders," in *Proceedings of the IEEE international conference on computer vision*, 2015, pp. 4633–4641.
- [36] A. Graves and N. Jaitly, "Towards end-to-end speech recognition with recurrent neural networks," in *International Conference on Machine Learning*, vol. 14, 2014, pp. 1764–1772.
- [37] K. Zhang, W.-L. Chao, F. Sha, and K. Grauman, "Video summarization with long short-term memory," in *European conference on computer vision*, 2016, pp. 766–782.
- [38] B. A. Olshausen and D. J. Field, "Sparse coding of sensory inputs," *Current opinion in neurobiology*, vol. 14, no. 4, pp. 481–487, 2004.
- [39] A. Ng, "Sparse autoencoder," *CS294A Lecture notes*, vol. 72, no. 2011, pp. 1–19, 2011.
- [40] J. Han, D. Zhang, X. Hu, L. Guo, J. Ren, and F. Wu, "Background prior-based salient object detection via deep reconstruction residual," *IEEE Transactions on Circuits and Systems for Video Technology*, vol. 25, no. 8, pp. 1309–1321, 2015.
- [41] X. Liang, S. Liu, Y. Wei, L. Liu, L. Lin, and S. Yan, "Towards computational baby learning: A weakly-supervised approach for object detection," in *Proceedings of the IEEE international conference on computer vision*, 2015, pp. 999–1007.
- [42] X. Wang and A. Gupta, "Unsupervised learning of visual representations using videos," in *Proceedings of the IEEE international conference on computer vision*, 2015, pp. 2794–2802.
- [43] X. Liang, Y. Wei, L. Lin, Y. Chen, X. Shen, J. Yang, and S. Yan, "Learning to segment human by watching youtube," *IEEE transactions on pattern analysis and machine intelligence*, vol. 39, no. 7, pp. 1462–1468, 2017.
- [44] Y. Xiang, A. Alahi, and S. Savarese, "Learning to track: Online multi-object tracking by decision making," in *Proceedings of the IEEE international conference on computer vision*, 2015, pp. 4705–4713.
- [45] R. Girshick, "Fast r-cnn," in *Proceedings of the IEEE international conference on computer vision*, 2015, pp. 1440–1448.
- [46] M. Everingham, L. Van Gool, C. K. I. Williams, J. Winn, and A. Zisserman, "The PASCAL Visual Object Classes Challenge 2012 (VOC2012) Results," <http://www.pascal-network.org/challenges/VOC/voc2012/workshop/index.html>.
- [47] M. A. Smith and T. Kanade, "Video skimming and characterization through the combination of image and language understanding," in *Proceedings of the 1998 International Workshop on Content-Based Access of Image and Video Databases*, 1998, pp. 61–70.
- [48] D. Li, J.-B. Huang, Y. Li, S. Wang, and M.-H. Yang, "Weakly supervised object localization with progressive domain adaptation," in *Proceedings of the IEEE Conference on Computer Vision and Pattern Recognition*, 2016, pp. 3512–3520.
- [49] J. Deng, W. Dong, R. Socher, L.-J. Li, K. Li, and L. Fei-Fei, "Imagenet: A large-scale hierarchical image database," in *Proceedings of the IEEE Conference on Computer Vision and Pattern Recognition*, 2009, pp. 248–255.
- [50] K. He, X. Zhang, S. Ren, and J. Sun, "Deep residual learning for image recognition," in *Proceedings of the IEEE Conference on Computer Vision and Pattern Recognition*, 2016, pp. 770–778.
- [51] O. Russakovsky, J. Deng, H. Su, J. Krause, S. Satheesh, S. Ma, Z. Huang, A. Karpathy, A. Khosla, M. Bernstein, A. C. Berg, and L. Fei-Fei, "Imagenet large scale visual recognition challenge," *International Journal of Computer Vision*, vol. 115, no. 3, pp. 211–252, 2015.
- [52] Y. Li and B. Merialdo, "Multi-video summarization based on videommr," in *Proceedings of the IEEE International Workshop on Image Analysis for Multimedia Interactive Services*, 2010, pp. 1–4.
- [53] S. E. F. De Avila, A. P. B. Lopes, A. da Luz, and A. de Albuquerque Araújo, "Vsumm: A mechanism designed to produce static video summaries and a novel evaluation method," *Pattern Recognition Letters*, vol. 32, no. 1, pp. 56–68, 2011.
- [54] K. Cho, B. Van Merriënboer, C. Gulcehre, D. Bahdanau, F. Bougares, H. Schwenk, and Y. Bengio, "Learning phrase representations using rnn encoder-decoder for statistical machine translation," *arXiv preprint arXiv:1406.1078*, 2014.
- [55] D. Zhang, D. Meng, and J. Han, "Co-saliency detection via a self-paced multiple-instance learning framework," *IEEE transactions on pattern analysis and machine intelligence*, vol. 39, no. 5, pp. 865–878, 2017.
- [56] D. Zhang, J. Han, C. Li, J. Wang, and X. Li, "Detection of co-salient objects by looking deep and wide," *International Journal of Computer Vision*, vol. 120, no. 2, pp. 215–232, 2016.
- [57] J. Zhang, Z. Lin, J. Brandt, X. Shen, and S. Sclaroff, "Top-down neural attention by excitation backprop," in *European Conference on Computer Vision*. Springer, 2016, pp. 543–559.
- [58] Y. Yuan, X. Liang, X. Wang, D.-Y. Yeung, and A. Gupta, "Temporal dynamic graph lstm for action-driven video object detection," *arXiv preprint arXiv:1708.00666*, 2017.
- [59] X. Liang, L. Lee, W. Dai, and E. P. Xing, "Dual motion gan for future-flow embedded video prediction," *arXiv preprint arXiv:1708.00284*, 2017.